Sensors and Materials, Vol. 19, No. 8 (2007) 465–476
MYU Tokyo

S & M 0697

Characteristics of Transcutaneous pCO_2 Gas Sensor Based on LiF Glass Using Soft Lithography

Hyang-Yi Bang, Kyung-Chan Kim[1], Byoung-Ho Kang[1], Do-Eok Kim[1], Nyeon-Sik Eum[2], Dae-Hyuk Kwon[3], Eun-Jong Cha[4] and Shin-Won Kang[5,*]

Department of Sensor and Display Engineering, Kyungpook National University, 1370 Sankyuk-dong, Bukgu, Daegu 702-701, Korea
[1]Department of Electronic Engineering, Kyungpook National University, 1370 Sankyuk-dong, Bukgu, Daegu 702-701, Korea Korea
[2]Department of Agriculture and Biological Engineering, Purdue University, 225 S, University Street, West Lafayette, IN, 47907, U.S.A
[3]School of Electronic Information & Communication Engineering, Kyungil University, 33 Buho-ri, Hayang-up, Gyeongsan-si, Gyeongsang buk-do 712-702, Korea
[4]Department of Biomedical Engineering, Chungbuk National University, 410 SungBong-Ro, Heungduk-gu, Cheongju, Chungbuk 361-763, Korea
[5]School of Electrical Engineering and Computer Science, Kyungpook National University, 1370 Sankyuk-dong, Bukgu, Daegu 702-701, Korea

(Received May 8, 2007; accepted September 7, 2007)

Key words: pCO_2, noninvasive, transcutaneous, NDIR, IR spectroscopy

In this study, we developed a noninvasive optical transcutaneous partial pressure of carbon dioxide, pCO_2, monitoring system by nondispersive infrared, NDIR. The objective of this system is to detect CO_2 from the outer skin and not by an arterial blood-sampling method. There are several advantages of this system, such as short analysis time and potential for real-time monitoring. This measurement system is composed of an IR lamp, a pyroelectric sensor including a 4.26 μm optical filter, an optical gas reaction chamber, and a signal processing circuit. The pass length of the optical reaction chamber is fixed at 1 mm by soft lithography because we considered that CO_2 gas is released from the human body. The fabricated pCO_2 monitoring system shows a sensitivity of 6.50×10^{-6} absorbance/ppm in an arterial-blood CO_2 concentration region of 0 to 5,000 ppm, is controlled using a mass flow controller (MFC), and has very fast response characteristics. We consider that this proposed system can be used in the optical-biosensor field for medical diagnosis, such as a pCO_2 monitoring system, a capnograph system for $EtCO_2$ analysis, and for environmental monitoring systems.

*Corresponding author: e-mail: swkang@knu.ac.kr

1. Introduction

The analysis of the partial pressure of carbon dioxide in arterial blood, pCO_2, is of great significance in medical diagnosis because pCO_2 is an indicator of alveolus ventilation and the acid-base balance of the human body. In particular, the continuous monitoring of arterial pCO_2 is essential for surgical and serious patients who depend on an artificial ventilator. However, the blood-sampling method has restrictions, which make it very invasive to patients, and needs much time for analysis because blood is directly obtained from the human body. In other cases of emergency in which patients require noninvasive analysis, arterial pCO_2 is inferred from end-tidal carbon dioxide, $EtCO_2$, analysis, which does not accurately determine the arterial pCO_2,[1] and is very troublesome because patients should breathe through a catheter. On the other hand, there is a report showing that transcutaneous pCO_2 measurement results agree with those of arterial blood pCO_2 measurement, which is determined by blood-sampling method.[2] Moreover, it has merits such as the arterial pCO_2 in a capillary vessel can be measured in real time.

Therefore, in this study, we fabricated a noninvasive optical transcutaneous pCO_2 gas sensor that functions according to the nondispersive infrared, NDIR,[3,4] method, which could be used as a real-time monitoring system, the principle of which is that infrared rays of a specific wavelength are absorbed by CO_2 gas. Figure 1 shows a schematic of the arterial-venous blood system in which CO_2 gas is produced by local tissue metabolism and released from the blood as it flows through the capillaries near the skin surface.[5] This real-time monitoring system will be available for the easy estimation of

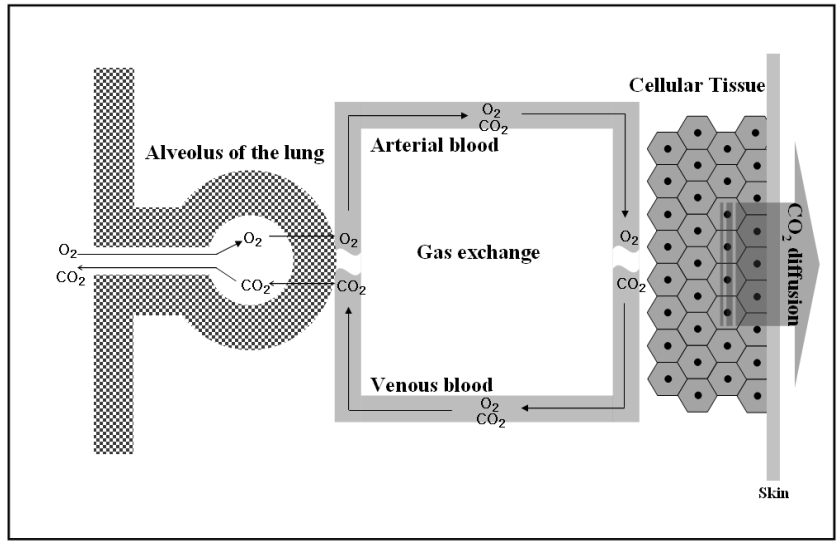

Fig. 1. Schematic diagram of arterial-venous blood system.

the patient's health condition, has minimum impact on the patients, and is the simplest method evaluation method for use in any medical office, emergency room, operating room, and even at home.

2. Materials and Methods

2.1 *Theory*

2.1.1 *IR spectroscopy*

Most gas detection systems use the NDIR method, in which all the light passes through a simple gas sample cell and filtered immediately through the optical filter before a detector, as shown in Fig. 2. This method is characterized by high optical transmission efficiency and long effective optical pass length of the reflection inside the sample gas cell. The absorption of this gas molecule causes changes in dipole moment because of the vibrations and rotations within a molecule. As the changes in dipole moment become bigger, the absorption of infrared ray increases. In particular, CO_2 gas exhibits very strong absorption bands in the 2.7 μm and 4.26 μm regions of the IR spectrum[6] as shown in Fig. 3. At 4.26 μm, no other atmospheric gases can be detected apart from CO_2 gas. This wavelength is appropriate for sensing CO_2 gas.

Therefore, the gas molecular absorbance that appears in the infrared ray spectra provides information on the gas molecule that we want to detect. This is an important clue similar to a human's fingerprint.

2.1.2 *Beer-Lambert's law*

The proposed pCO_2 analysis system using IR spectroscopy method is based on the Beer-Lambert law.[7] The ratio of the transmitted intensity (I_t) to the initial intensity (I_0) of the IR radiation through an absorbing medium at a particular frequency relates

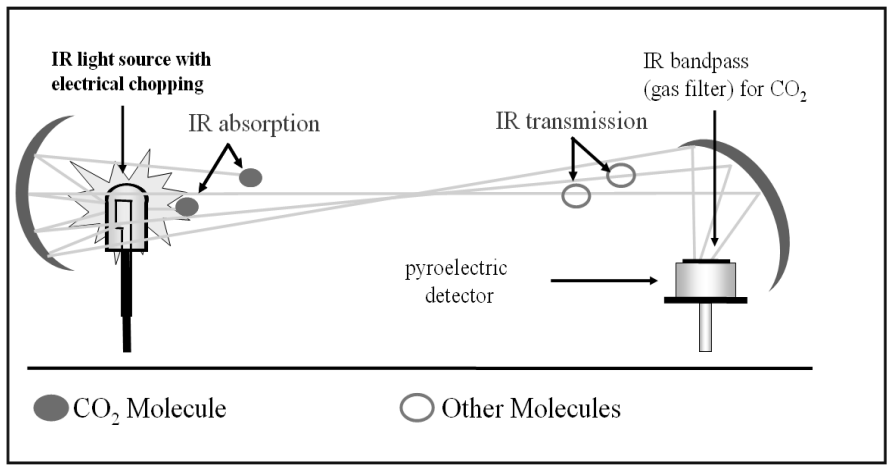

Fig. 2. Schematic diagram of NDIR method.

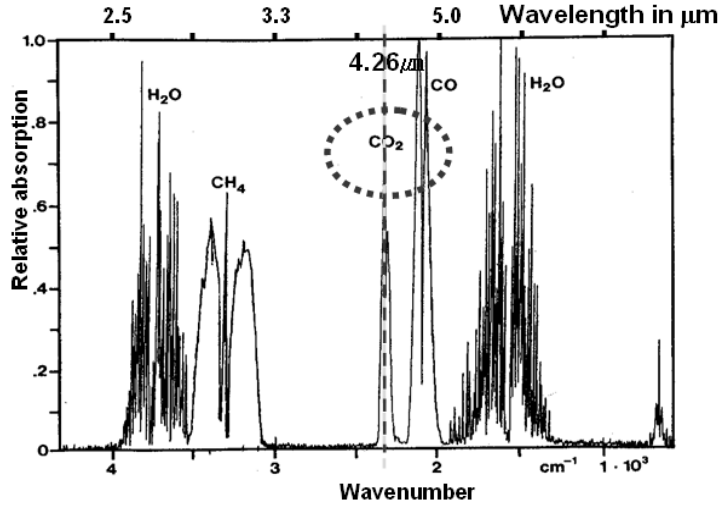

Fig. 3. IR Spectrum of CO_2.

exponentially to the transition line strength S_i [cm^2atm^{-1}], line-shape function φ [cm], total pressure P [atm], absorption coefficient for concentration ϵ [$M^{-1}cm^{-1}$], material concentration C [Mol], and path length L [cm].

$$I_t = I_0 \exp(-S_i \varphi \in PCL) \tag{1}$$

The IR intensity can be converted to an absorbance $A(\alpha)$ and is related to the transition parameters by

$$A(\alpha) = -\ln(I_t/I_0) = S_i \varphi \in PCL \tag{2}$$

The absorption coefficient is defined as:

$$\alpha(v) = S_i \varphi \in \tag{3}$$

From eq. (2), the absorption $A(\alpha)$ can be defined as:

$$A(\alpha) = \alpha(v) PCL \tag{4}$$

In this equation, the absorption $A(\alpha)$ is linearly proportional to the concentration C of the measured gas, path length L and pressure P.[8,9]

2.2. *Experiment system*

In this study, the proposed system is an optical system that detects the selected wavelength in the range of mid-IR radiated from a light source without using a prism

or diffraction grating by NDIR method. Figure 4 shows a schematic of the fabricated system. This optical system is composed of a light source that provides a mid-IR and an optical reaction chamber to make the vibration energy level of the sample gas change in this part, a detector that detects the intensity of light, and a signal processing circuit to amplify a microsignal.

First of all, the light source used is a tungsten filament lamp (IRL715, Perkin Elmer, USA) that emits a stable infrared wavelength in the 2–4.4 μm range, while an electrical chopper provides a frequency of 1.2 Hz, and it is embedded in a reflector to collect light. The detector is a pyroelectric sensor (LHi 807TC, Heimann, Germany) that is used as a thermal detector which has uniform detection sensitivity in the mid-IR range. The voltage sensitivity, absorber size, and detection sensitivity of this pyroelectric sensor are shown in Table 1. Also, this detector selectively detects a single wavelength due to a 4.26 μm optical band-pass filter in front. The signal processing circuit consists of a signal-amplifying part, and analog-to-digital and digital-to-analog conversion parts as shown in Fig. 5. The signal-amplifying part is designed by amplifying and rectifying an output

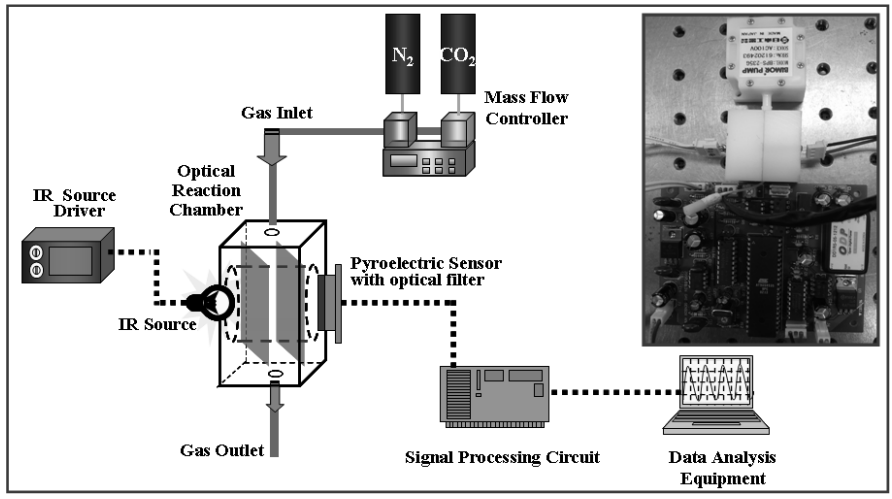

Fig. 4. Schematic diagram of entire measurement system.

Table 1
Characteristics of pyroelectric sensor.

Series-Pyroelecteric sensor	Type of sensor	Housing	Absorber size [mm^2]	Sensitivity [V/M]	Detection sensitivity [cmHz$^{0.5}$/W]
LHi 807 TC	Single	TO 5	1.5×1.5	320	16×10^7

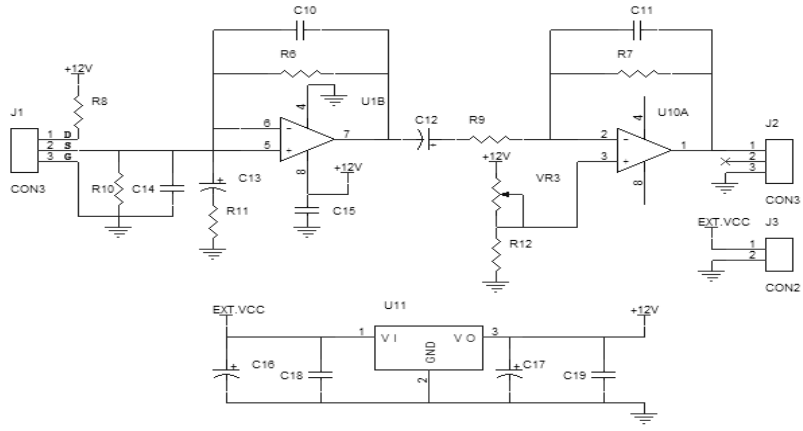

(a)

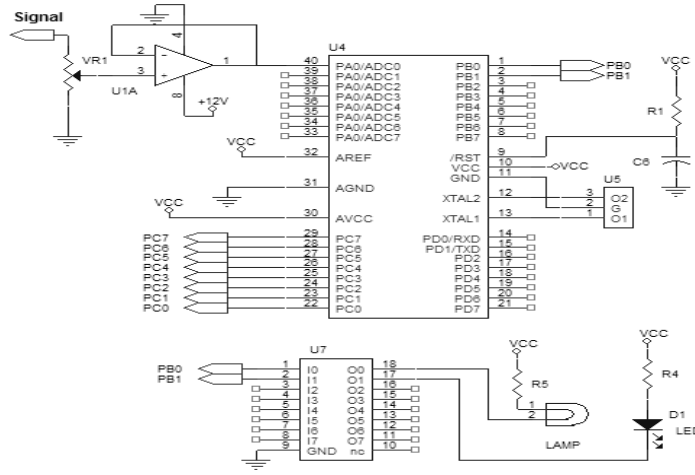

(b)

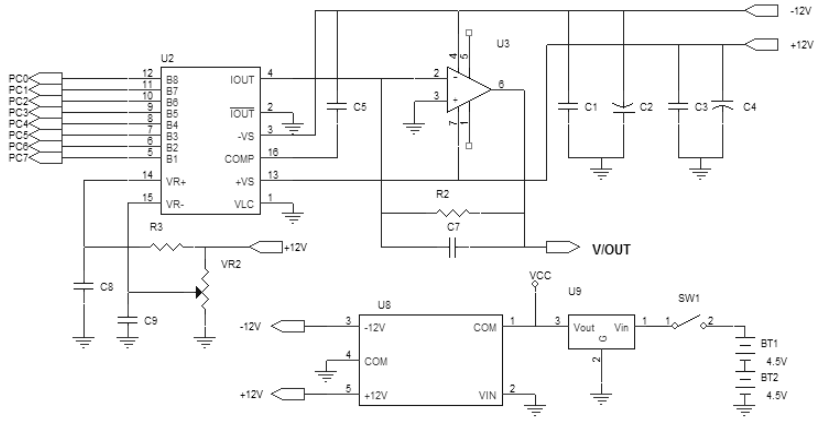

(c)

Fig. 5. Signal processing circuit for output signal. (a) Signal amplifying part. (b) Analog-to-digital conversion part. (c) Digital-to-analog conversion part.

signal from the pyroelectric sensor which changes in detail as CO_2 reacts at the 4.26 μm wavelength.[10] The analog-to-digital and digital-to-analog conversion parts are designed to convert the analog signal from the signal-amplifying part to a digital signal. The variation of the CO_2 concentration can be easily determined using this final output signal. Then, the optical reaction chamber is designed by a 1 mm optical path length and 64 μl volumes, considering that a very small amount of CO_2 gas is released from the skin.

Figures 6(a) and 6(b) show fabrication processes of the optical reaction chamber. The Si-based optical reaction chamber is fabricated by photolithography using etching

(a)

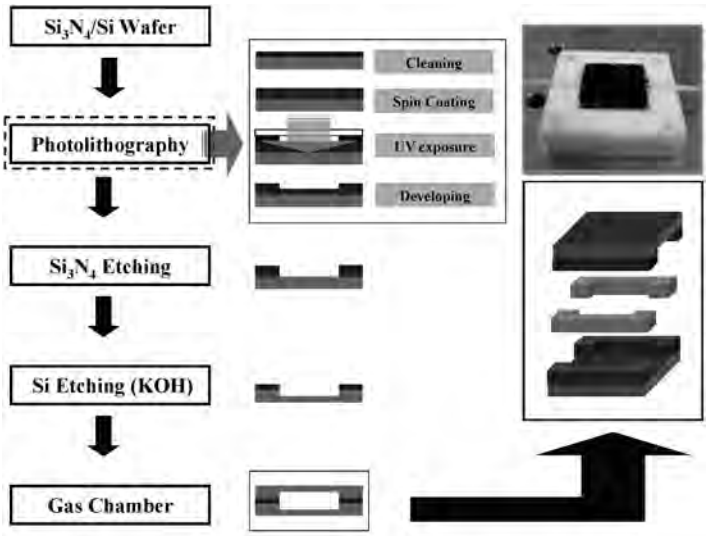

(b)

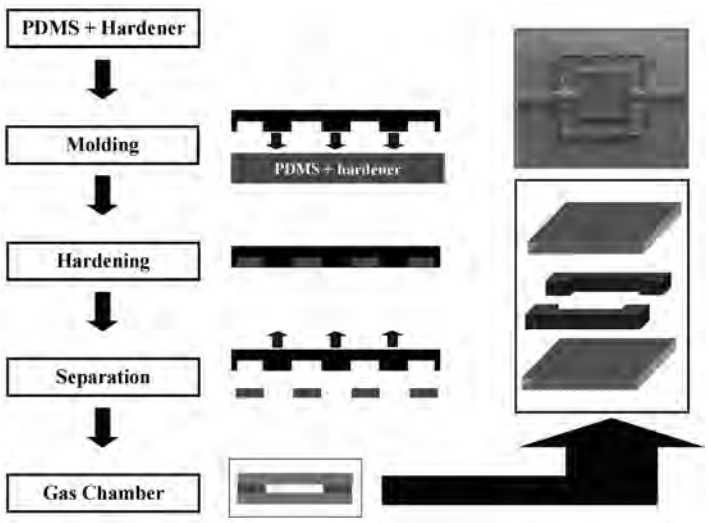

Fig. 6. Process sequences for fabrication of optical reaction chamber. (a) Process flow of Si-based optical reaction chamber. (b) Process flow of LiF-based optical reaction chamber.

and bonding processes.[10] To make a 1 mm optical path length, two Si substrates are etched up to 300 μm via wet etching. Then, a Si-supporting layer is bonded between two Si substrates. This process, however, makes the surface of the Si substrate rough and causes a decrease in the IR transmittance rate. Therefore, LiF glass, which is used as prism material,[11] is used for fabricating the optical reaction chamber because it has a very high optical transmittance compared to Si substrate, as shown in Fig. 7. This LiF-based optical reaction chamber has a 1 mm optical path length as determined by soft lithography, which results in a short fabrication process time. Also, the surface of the LiF glass is not rough because soft lithography does not require an etching process. It denotes that the LiF-based optical reaction chamber can be used to increase process efficiency and detection efficiency. Also, the LiF-based optical reaction chamber can be used as a thermally and chemically stable acetal stamp master to define the 1 mm optical path length by soft lithography. These two types of fabricated optical reaction chamber and unification style are shown in Fig. 8. Finally, the light source, the optical detector and the optical reaction chamber are embedded as a single teflon unit to intercept the effect of outside light, temperature, moisture, and others.

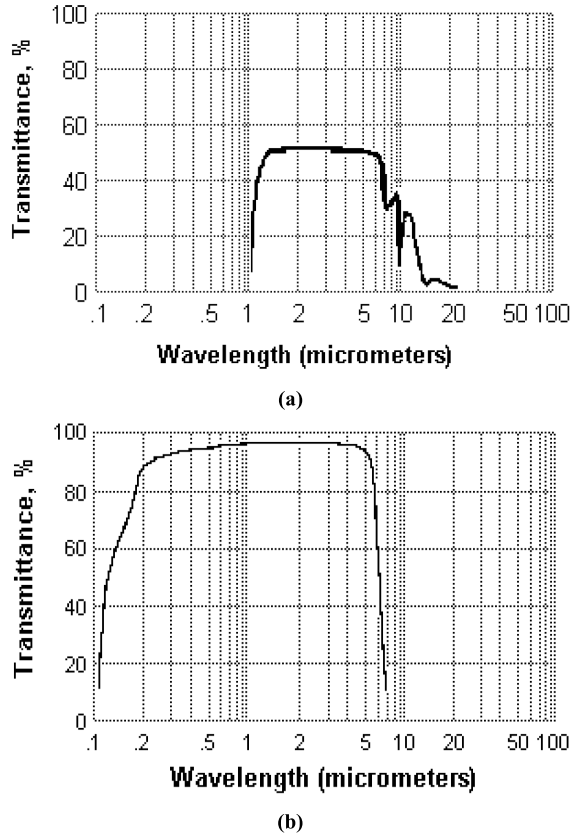

Fig. 7. IR transmittance of each substrate. (a) Si and (b) LiF.

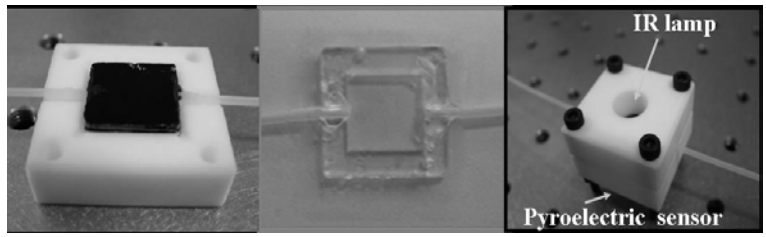

Fig. 8. Each fabricated optical reaction chamber and unification unit with Teflon.

3. Result

The IR transmittance of the two types of fabricated optical reaction chamber was measured using an FT-Infrared Spectrophotometer (Mattson Instruments, Inc., Galaxy 7020A) and the results are shown in Fig. 9. This figure shows that the LiF-based optical reaction chamber has approximately 70% IR transmittance compared with the Si-based optical reaction chamber, which has 35% IR transmittance in the 4.26 μm wavelength. Figure 10 shows the absorbance according to the CO_2 concentration. This figure shows the absorbance in the arterial pCO_2 concentration region, 0–5,000 ppm, after blowing CO_2 gas into each optical reaction chamber using MFC (Mass Flow Controller, P.J. KODIVAC, Japan). The variation results of the absorbance are 3.78×10^{-6} and 6.50×10^{-6} absorbance/ppm in the arterial pCO_2 concentration region. As a result, the LiF-based optical reaction chamber has higher efficiency, which increased by 65% compared with the Si-based optical reaction chamber. Also, Figs. 11(a) and 11(b) show the output voltage detected through the signal processing circuit when CO_2 gas runs into the LiF-based optical reaction chamber in the $EtCO_2$ concentration and arterial pCO_2 concentration regions, respectively. This result corresponds to the Beer-Lambert's law.

On the basis of the fundamental results, an experiment system was equipped for a simulated clinical demonstration. Figure 12 shows a schematic of the entire system that is composed of a skin-mounted pad warming the skin at approximately 40°C, and based on the characteristics of high solvency and diffusivity of CO_2 gas into the skin,[12,13] and a vacuum pump that moves the CO_2 gas diffused from the skin into the optical reaction chamber.

As shown in Fig. 13, a 60 mV response characteristic was obtained in the region of 3,500 ppm CO_2 concentration after the skin-mounted pad was mounted on a wrist of a non-operator to collect CO_2 gas from the capillary vessel. This result is equivalent to 10% of the $EtCO_2$ concentration region as we calculated. Also, the response characteristic was very fast at less than 100 ms.

4. Discussion

In this study, the most important part of the fabricated system is the optical reaction chamber into which a small amount of CO_2 gas is exhausted. In accordance with this, we could fabricate the optical reaction chamber by soft lithography. This method makes

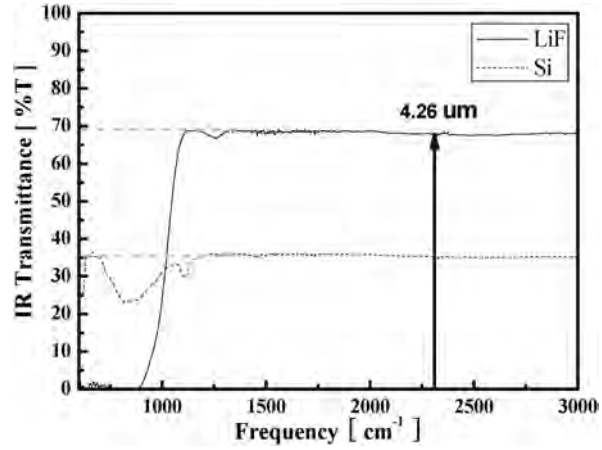

Fig. 9. IR transmittances of Si-based optical reaction chamber and LiF-based optical reaction chamber.

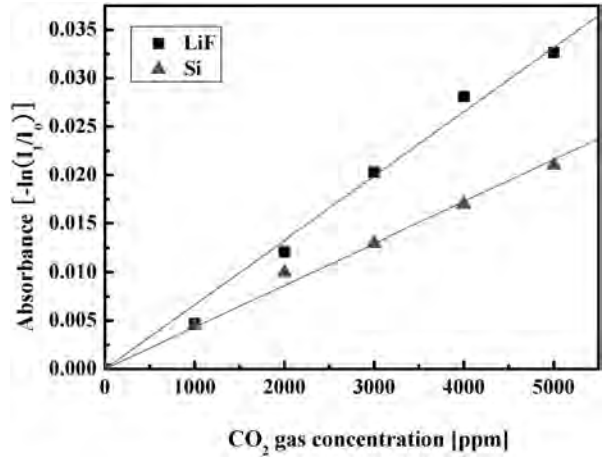

Fig. 10. Absorbance of each chamber in arterial-blood CO_2 concentration region.

the fabrication of the optical reaction chamber very easy and precise. Moreover, the LiF glass has a very high transmittance in the 4.26 μm region of the IR spectrum compared with Si wafer. Therefore, we could obtain a better IR absorbance depending on the CO_2 concentration.

On the basis of this experiment, unless there are additional studies showing a more accurate correlation of results using blood-sampling method and interference between moisture and different types of gases, this optical transcutaneous pCO_2 gas sensor can be used as a small tool in the biomedical field, atmospheric environmental monitoring field and at home.

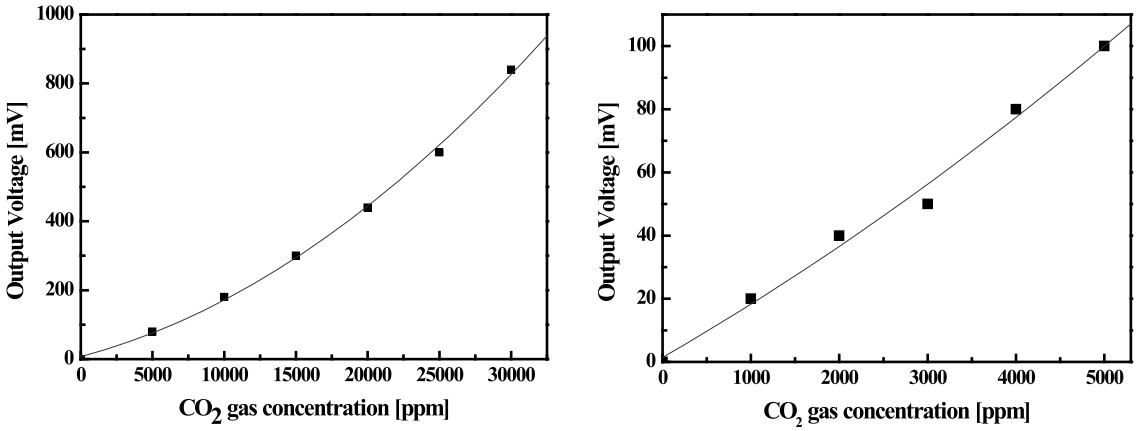

Fig. 11. Output voltage according to CO_2 concentration using LiF-based optical reaction chamber. (a) Output voltage according to $EtCO_2$ concentration region. (b) Output voltage according to pCO_2 concentration region.

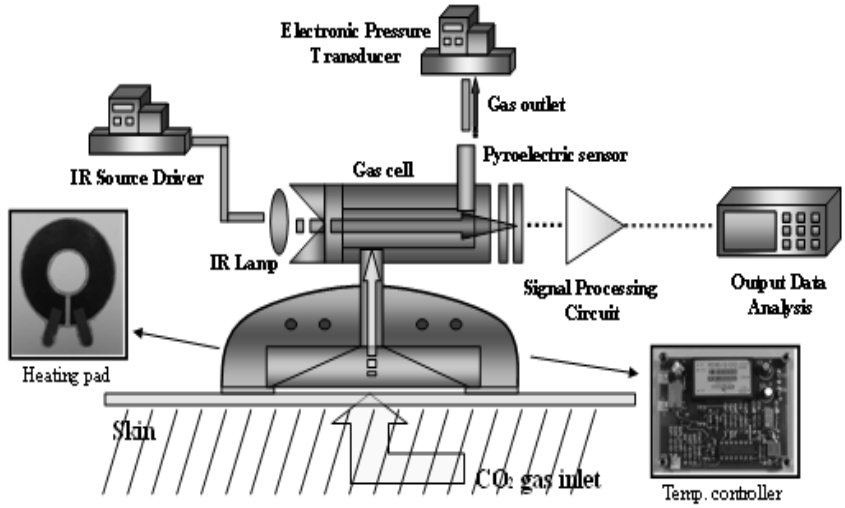

Fig. 12. Schematic diagram of detection system including skin mount pad.

Acknowledgement

This study was supported by a Grant from the Korea Health 21 R&D Project, Ministry of Health & Welfare, Republic of Korea.

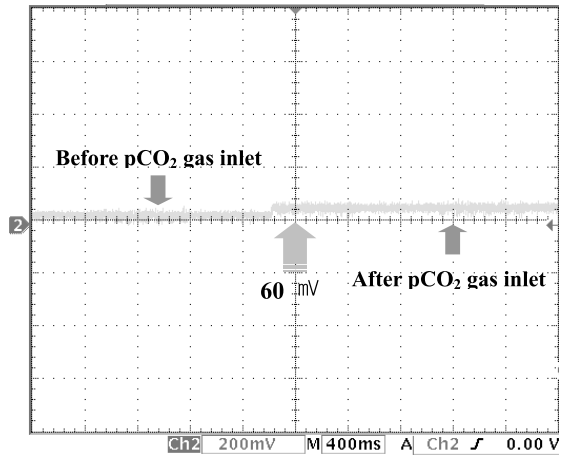

Fig. 13. Response characteristic of pCO_2 by using skin mount pad.

References

1 J. Griffin, B. E. Terry, R. K. Burton, T. L. Ray, B. P. Keller and *et al.*: BJA. **91** (2003) 498.
2 V. Rosner, B. Hannhart, F. Chabot and J. M. Polu: Eur Respir J. **13** (1999) 1044.
3 G. Zhang, J. Lui and M. Yuan: Opt. Eng. **39** (2000) 2235.
4 E. Wagner, R. Dandliker and K. Spenner: Sensors: Optical Sensors (VCH press, New York, 1991) Chap. 12.
5 F. S. Grodins and M. S. Yamashiro: Respiratory Function of the Lung and Its Control (Macmillan Pub Co, England, 1982) Chap. 1.
6 A. Verdin: Gas Analysis Instrumentation (The Macmillian Press, London, 1973) p. 67.
7 M. E. Webber: Doctoral thesis, Stanford University, 2001.
8 H. Ahlberg, S. Lundqvist, R. Tell and T. Andersson: Proc. SPIE **2112** (1994) 118.
9 N. J. Choi: Masteral thesis, Kyungpook National University, 1998.
10 D. E. Kim, Hwan Joo Lee and *et al.*: Sensors and Materials. **18** (2005) 253.
11 J. P. Marangos, R. C. M. Learner and *et al.*: Journal of Modern Optics. **39** (1992) 2445.
12 W. Kim, B. J. Oh, J. Y. Ahn, Y. J. Lee, Y. Koh and *et al.*: Journal of the Korean Society of Emergency Medicine. **15** (2004) 446.
13 P. Cox and J. D Tobias: Journal of Minimal Access Surgery. **3** (2007) 12.